Microchemical Journal 200 (2024) 110345

Contents lists available at ScienceDirect

Microchemical Journal

journal homepage: www.elsevier.com/locate/microc

Bioinspired host-tailored polymers based on molecular imprinting for cytokine assessment

Bianca Ferreira [a,b], Miguel Correa-Duarte [c,d], Arcelina Marques [e], Felismina Moreira [a,b,f], Gabriela Martins [a,b,f,*]

[a] BioMark@ISEP, School of Engineering of Polytechnique School of Porto, Porto 4200-072, Portugal
[b] LABBELS/CEB, Centre of Biological Engineering, University of Minho, Braga, Braga 4710-057, Portugal
[c] CINBIO, Universidade de Vigo, Vigo 36310, Spain
[d] Biomedical Research Networking Center for Mental Health (CIBERSAM), Southern Galicia Institute of Health Research (IISGS), Vigo 36310, Spain
[e] CIETI, School of Engineering, Polytechnic of Porto, Porto 4200-072, Portugal
[f] LabRISE@CIETI, School of Engineering of Polytechnique School of Porto, Porto 4200-072, Portugal

ARTICLE INFO

Keywords:
Cyclodextrins
Electropolymerization
Molecular imprinting
Electrochemical
Interleukin-6

ABSTRACT

Molecular imprinting undergone a substantial boost driven by the awareness of molecularly imprinted polymers (MIPs)-ligand recognition skills. In particular, the introduction of natural-based compounds like cyclodextrins into the structural scaffold of synthetic recognition elements attracted great importance as a novel route to design more friendly-environments for protein binding, while promoting higher selectivity features. Herein, carbon electrodes doped with platinum nanoparticles supported on multiwalled carbon nanotubes and functionalized with polyallylamine (MWCNTs-PAH/Pt) were electrochemically modified with an imprinted sensing layer of poly(β-cyclodextrin-pyrrole) (poly(β-CD-Py)) towards interleukin 6 (IL-6) monitoring. The analytical performance of the biosensor was evaluated by using Cyclic Voltammetry and Electrochemical Impedance Spectroscopy techniques. Along the assembly, experimental parameters like nanomaterial deposition, monomer-protein concentrations and template removal solutions were carefully optimized and discussed. Furthermore, the electrodeposited film was characterized in terms of composition, morphology and structure using scanning electron microscopy (SEM) and Raman spectroscopy. Under optimal conditions, the developed sensor was able to rebind IL-6 over a wide linear range [1 pg/mL – 100 ng/mL], displaying high sensitivity, quick electrochemical response, and specific binding of the target molecule. Overall, this work reported the relevance of using host-guest complexes directly embedded in polymeric chains to generate newly controlled electrochemical sensors holding great potential for protein biosensing.

1. Introduction

Molecular imprinting technology has received increasing attention in the last decades, particularly regarding its application for biomolecules detection, diagnostic testing and also, as a promising therapeutic tool [1–5]. Molecularly imprinted polymers (MIPs) consist in artificially-made polymeric structures with the ability to recognize and bind to a specific target molecule [6,7]. The synthesis of these highly sensitive recognition elements involves a polymerization reaction using a functional monomer in the presence of a target template molecule. Afterwards, to create a three-dimensional imprinted cavity, complementary to the template in terms of size, shape and functional groups, the imprinted molecule is extracted from the polymeric matrix, without damaging the polymer structure [8]. The use of MIPs in the design of chemical and electrochemical sensing devices has been extensively explored due to their facile and quick fabrication, high mechanical and storage stability, inexpensive cost, and excellent sensitivity features [9–11]. Nevertheless, a full understanding of the interaction peculiarities between the target molecule of interest (analyte) and the imprinted (polymer) site created within the MIP material is still highly relevant. Hence, the formation of MIP structures using two different monomer species can generate, modulate, and enhance the diversity of the imprinted cavities, affecting their affinity characteristics and consequently, improving the selectivity and sensitivity features of the

* Corresponding author at: BioMark@ISEP, School of Engineering of Polytechnique School of Porto, Porto 4200-072, Portugal.
E-mail address: fvm.gabriela@gmail.com (G. Martins).

https://doi.org/10.1016/j.microc.2024.110345
Received 8 September 2023; Received in revised form 12 March 2024; Accepted 16 March 2024
Available online 17 March 2024

response.

In this context, cyclodextrins (CDs) and their derivatives have been largely employed as molecular recognition systems, specifically applied for the integration and construction of electrochemical sensing platforms. Particularly, β-cyclodextrin (β-CD) is a naturally occurring cyclic oligosaccharide consisting of seven glucose units. It possesses a toroidal shape characterized by an inner hydrophobic cavity and an outer hydrophilic shell [12,13]. This singular structure is responsible for the entrapment of a wide variety of organic and inorganic compounds in solution phase, which results in the formation of a stable self-assembly host-guest complex [14]. According to this host-guest interaction, β-CDs enable high molecular selectivity and enantioselectivity since various organic, inorganic, and biological guest molecules can be targeted because of the selective binding in the hydrophobic inner cavity. For this reason, the inclusion complex between hydrophobic biomolecules like proteins, drugs and other guest targets and the cavity of CDs makes these structures promising candidates for drug delivery systems, diagnosis, and therapeutic purposes [14,15]. Furthermore, molecular interactions involving CDs are widely acknowledged for their natural inspiration from certain processes found in biological systems, such as, enzyme-substrate interactions and receptor-ligand recognition. Thus, innovation at this level can be achieved through the incorporation of natural-based β-CDs in the assembly of synthetic recognition structures, not only to promote selectivity characteristics, but also to create a more friendly-environment for protein binding, avoiding conformational and denaturation issues.

A common approach employed during the construction of different electrochemical sensors has been the use of β-CD as a modifying agent [16]. Recently, remarkable efforts have been made regarding the synthesis of CD-graphene hybrid materials. In this case, the fabricated materials resulted in the combination of superior electrochemical properties of graphene with the CD's high supramolecular recognition capabilities [17]. As an alternative to the immobilization approach of chemically modified CDs, electropolymerization has been also successfully established for the incorporation of CDs directly onto the sensing surfaces. Electrochemical polymerization provides a straightforward, environmentally friendly, and efficient pathway that can result in two distinct assemblies: (i) direct electrodeposition of CDs and (ii) entrapment of CDs in electrodeposited polymeric films. Zhang et al. explored the possibility of immobilization of β-CDs and L-arginine on carbon paste electrodes (CPEs) for electrochemical detection of fluoroquinolones [18]. The results showed that the obtained electrode presented an excellent electrocatalytic activity for the oxidation of ciprofloxacin target. Although some MIP sensors based on electrochemical polymerization of β-CD as the functional monomer in the presence of a template molecule have been accomplished [19], in some cases they require the application of a large potential window [-2.0; +2.5] V to assure a homogenous polymeric coating [20]. To overcome this limitation associated to the need of high energy, herein the proposed strategy consists in the integration of β-CDs with semiconducting polymers (SCP) in order to facilitate the growth of a responsive polymeric film and, simultaneously, taking advantage of the host-guest affinity properties. Due to their high charge mobility and tunable energy levels, SCPs can facilitate direct signal transduction in biosensors, which results in improved sensing capabilities. Thus, this work proposes a synergistic combination of the unique electronic properties of SCPs with CD's skills to create and tune high affinity recognition sites.

The utilization of pyrrole (Py) in the generation of MIPs has been widely investigated mostly due to its high stability, good biocompatibility, easy polymerization, and high conductivity performance [21,22]. Several MIP-based biosensors have been developed using poly(pyrrole) (PPy) as a smart scaffold for the detection of specific biomarkers of interest like pollutants [23,24], proteins [25], bacteria [26], aminoacids [27], antibiotics [28] among others. Despite the good electrochemical performance of PPy films, their properties can be greatly enhanced by the incorporation of nanomaterials into the surface of the electrodes. The use of nanostructured materials with high surface areas, such as, carbon nanotubes, graphene and metallic nanoparticles has received greater attention over the last decades [29,30]. Most of these materials exhibit faster analyte diffusion, higher binding capacities, and enhanced sensitivities that with suitable functionalization can trigger the adsorption of more template molecules on their surfaces, increasing the number of imprinted sites [31,32].

As the global population ages, the prevalence of neurodegenerative disorders like Alzheimer and Parkinson diseases has significantly increased, boosting technological efforts towards the development of novel, quick and early diagnostic tools. From the point-of-view of neuroinflammation, cytokines operate as neuromodulators, responsible for cell signalling, that regulate cell migration to the site of infection or injury as an immune response of the body [33]. Particularly, interleukin 6 (IL-6) is known as a main cytokine of inflammation, playing a central role in the host defence mechanism [34]. Presently, IL-6 detection employs diverse techniques such as high-performance liquid chromatography (HPLC) [35], mass spectrometry [36], capillary electrophoresis [37], fluorescence [38]. These methods have demonstrated remarkable sensitivity, achieving low limits of detection, with electrophoresis and fluorescence techniques achieving values as low as 0.1 fg/mL and 0.019 ng/mL, respectively. Although quite satisfactory in terms of sensitivity and selectivity performance, these methodologies present elevated costs, high consumption of time and organic solvents with complex operation protocols. Meanwhile, some electrochemical sensors have already been investigated for the determination of IL-6 but the great majority employs natural expensive recognition elements, such as, antibodies [39–41]. In this work, we were looking for a MIP-sensing platform which can be assembled through a more controllable methodology by incorporating β-CDs in Py-based electropolymerizable films for sensitive detection of IL-6 biomarker (Fig. 1). Furthermore, a nanocomposite material constituted by platinum nanoparticles supported on multiwalled carbon nanotubes and functionalized with polyallylamine (MWCNTs-PAH/Pt) was previously coated on the surface of carbon screen-printed electrodes (C-SPE) to improve polymer affinity and to enhance electron transfer.

2. Materials and methods

2.1. Reagents

All reagents were of analytical grade and used without further purification. Sulphuric acid (H_2SO_4, 95–97 %), citric acid ($C_6H_8O_7$), β-cyclodextrin (β-CD), interleukin-6 (IL-6, reference SRP3096, MW 21 kDa, 183 amino acids) recombinant protein and proteinase k were purchased from Sigma-Aldrich; potassium hexacyanoferrate III ($K_3[Fe(CN)_6]$), potassium hexacyanoferrate II ($K_4[Fe(CN)_6]$) trihydrate and dipotassium hydrogen phosphate (K_2HPO_4) from Riedel-de-Häen; potassium di-hydrogenophosphate (KH_2PO_4) from Panreac; oxalic acid ($C_2H_2O_4{\cdot}2H_2O$) from Merck; potassium chloride (KCl) from Normapur; sodium hydroxide (NaOH) from EKA; pyrrole (C_4H_5N, 98 %) from Alfa Aesar and human serum HN from PZ CORMAY S.A. The supporting electrolyte and the buffer solutions were prepared with ultrapure water Mili-Q laboratory grade. The pH measurements were conducted in a pH meter from Crison® Instruments (GLP21 model). All measurements were conducted at ambient temperature.

2.2. Apparatus

C-SPEs (Metrohm Dropsens, DRP-C110) were used as the conductive substrate, constituted by a carbon working electrode (WE, 4 mm diameter), a carbon counter electrode (CE) and a pseudo-reference silver electrode (RE). All experiments were conducted in triplicate under unstirred conditions at room temperature. Electrochemical measurements were conducted using a Metrohm Autolab potentiostat/galvanostat (PGSTAT204 with an FRA module), through a suitable interface

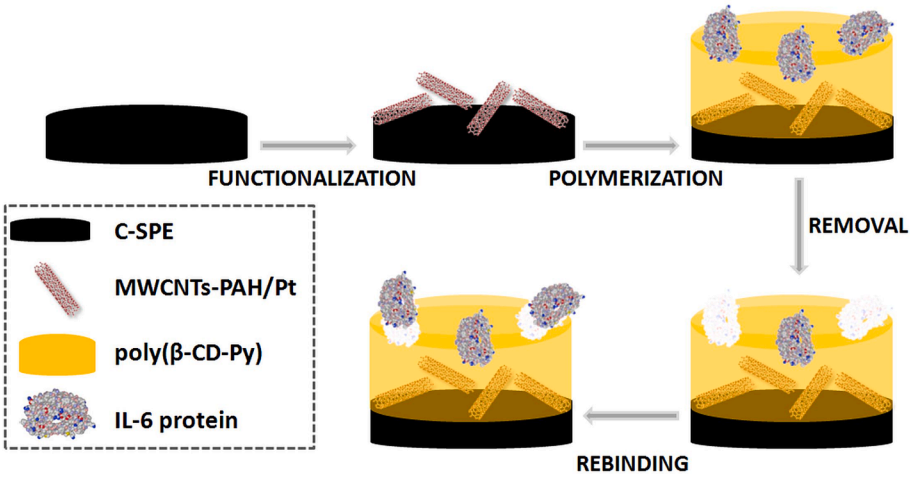

Fig. 1. Schematic representation regarding the fabrication process of electrosynthesized MIP on modified nanocomposite (MWCNTs-PAH/Pt) carbon screen-printed electrodes (C-SPE).

switch box (PCON from BioTid) and controlled by NOVA 2.1.4 software.

Chemical characterization regarding the modifications on the electrode surface were carried out by Raman spectroscopy using a ThermoScientific DXR Raman microscope system with a 785 nm excitation laser (operational conditions: 2 min of photobleach and 10 min of collect time). Data analysis was performed with OMNIC software.

Scanning Electron Microscopy (SEM) analysis was carried out to assess the morphology of the polymeric films on the electrode surface. This was conducted using a Carl Zeiss AURIGA Crossbeam SEM-FIB workstation, operating with a voltage of 5 kV coupled with the energy dispersive spectroscopy (EDS) detector.

2.3. Molecular visualization and simulation

To understand the structural interaction of IL-6 protein, the representation of surface electrostatic was constructed by employing the PDB files. Initially, the electrostatic potential representation was generated by converting the PDB file into a PQR file. Then, the file PDB2PQR v2.0.0 web service (https://nbcr-222.ucsd.edu/pdb2pqr_2.0.0) was created by using the isoelectric point for the entire protein by the PROPKA v3.0 web service (Poisson-Boltzmann). Lastly, the PQR file is processed using the APBS plugin within the Pymol software. This processing calculates the molecular surface and applies coloration based on the electrostatic potential variation, spanning from negative to positive ranges.

A molecular docking simulation study was performed by using AutoDock Vina free software (version 1.5.7), accompanied by AutoDock MGL Tools and Pymol, to predict binding conformations and estimate free energies for small molecule ligands interacting with macromolecular targets.

2.4. Biosensor fabrication

First, the C-SPEs were electrochemically treated in a 0.5 mol/L sulphuric acid solution using cyclic voltammetry (CV) over the potential range [-0.3; +1.5] V, at 50 mV/s, during 10 scans. Subsequently, the electrodes were rinsed with Milli-Q water and dried using a stream of nitrogen gas. The cleaned C-SPEs were functionalized with a layer of MWCNTs-PAH/Pt by performing sequential incubations in the WE, at different temperatures. This procedure was performed at least three times.

The MWCNTs-PAH/Pt were obtained following the same protocol developed by our team [42]. Briefly, carbon nanotubes (CNTs) were first functionalized with polyallylamine hydrochloride (PAH), a positively charged polyelectrolyte. Finally, the MWCNTs-PAH/Pt nanocomposite was obtained by means of the deposition of the previously synthesized platinum dendritic nanoparticles (Ptd-NPs) onto the surface of the PAH-functionalized CNTs.

For the electrosynthesis of the MIP-based poly(β-CD-Py) film, a mixture of β-CD (1 mM) and pyrrole (2.5 mM) prepared in 0.15 mol/L phosphate-citrate buffer at pH 5.0 was employed as the monomeric mixture in the presence of IL-6 protein target. Optimization experiments were conducted by testing different concentrations of β-CD (1.0 μg/mL and 0.1 μg/mL). The copolymer was electropolymerized in the modified WE through 30 scans of CV applied in a potential range of 0 to +1.8 V at 100 mV/s. Finally, the poly(β-CD-Py)/MWCNTs-PAH/Pt/C-SPE electrode was immersed in oxalic acid solution (0.5 M) for 3 h to leach out the IL-6 molecules from the polymeric matrix. Under the same conditions, the non-imprinted polymer (NIP) modified electrode was synthesized but without addition of IL-6 in the polymerization mixture.

2.5. Electrochemical assays

The electrochemical response of the MIP biosensor was recorded during all modification steps in 5 mM $K_3Fe(CN)_6/K_4Fe(CN)_6$ redox probe prepared in phosphate-citrate buffer solution (0.15 M, pH 5.0), employing CV and/or electrochemical impedance spectroscopy (EIS).

Calibration curves were obtained with IL-6 standard solutions with concentrations ranging from 1.0 pg/mL to 1.0 μg/ml in buffer solution and commercial human serum 100x diluted. The incubation time for IL-6 protein was set to 30 min before reading the redox probe using EIS technique.

3. Results and discussion

3.1. Characterization studies of the modified electrodes

As electrode modifiers, different nanocomposite structures have been widely incorporated directly into electrochemical platforms aiming for two purposes: enhancement of electronic transference and anchoring biological recognition elements [43]. Herein, previously synthetized MWCNTs-PAH/Pt material [42] was immobilized on a carbon electrode surface by physical adsorption. The initial step consisted in the cleaning of the transducer surface through a potential cycling in sulfuric acid to eliminate some organic contaminants that can be present in the electrode's surface and, simultaneously, the creation of vacant adsorption sites on the carbon layer more prompt to be later occupied. CV and EIS techniques were employed to investigate the electroactivity of the carbon surfaces before and after acidic electrochemical treatment (Fig. 2A and B). The acquired cyclic voltammograms

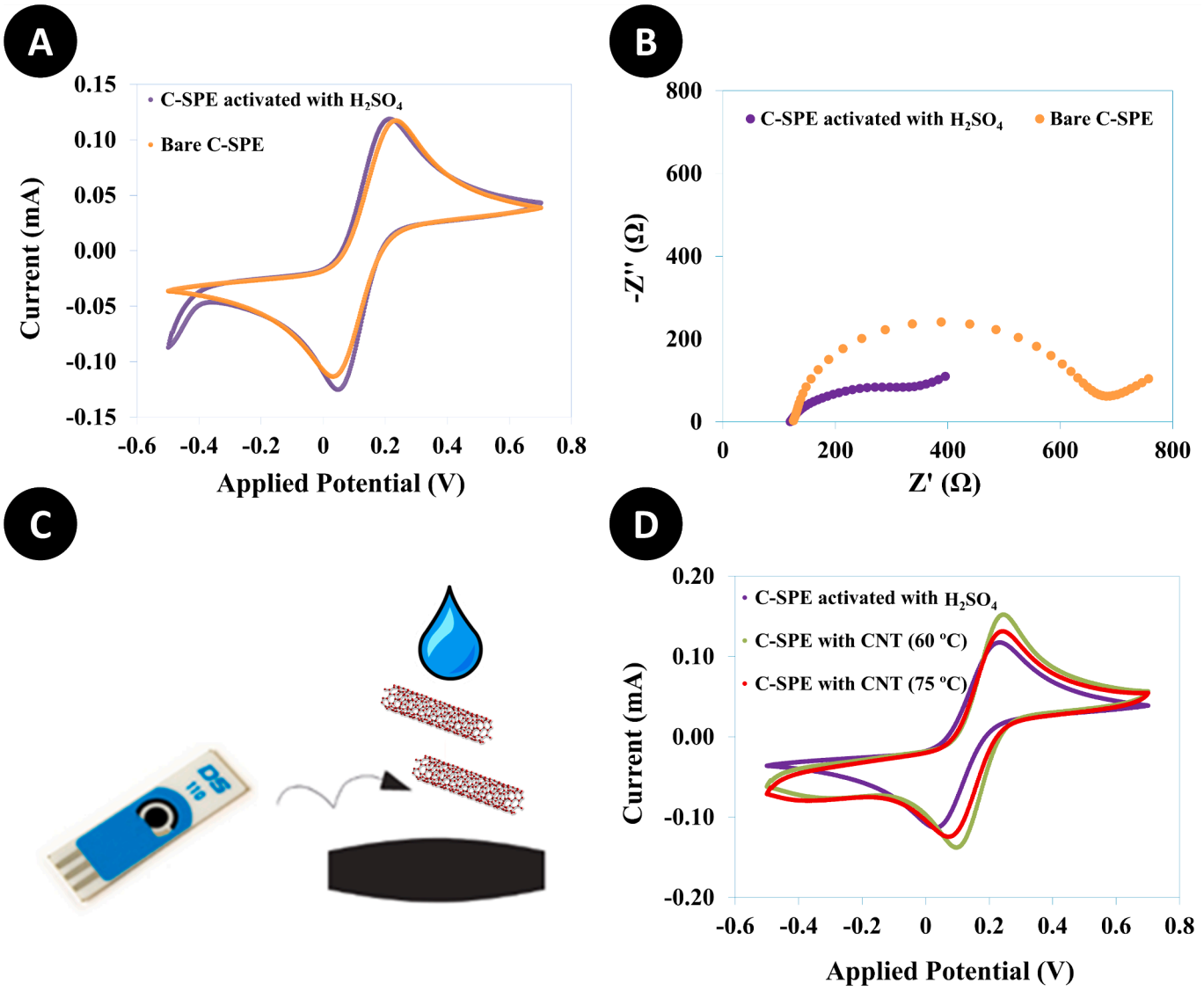

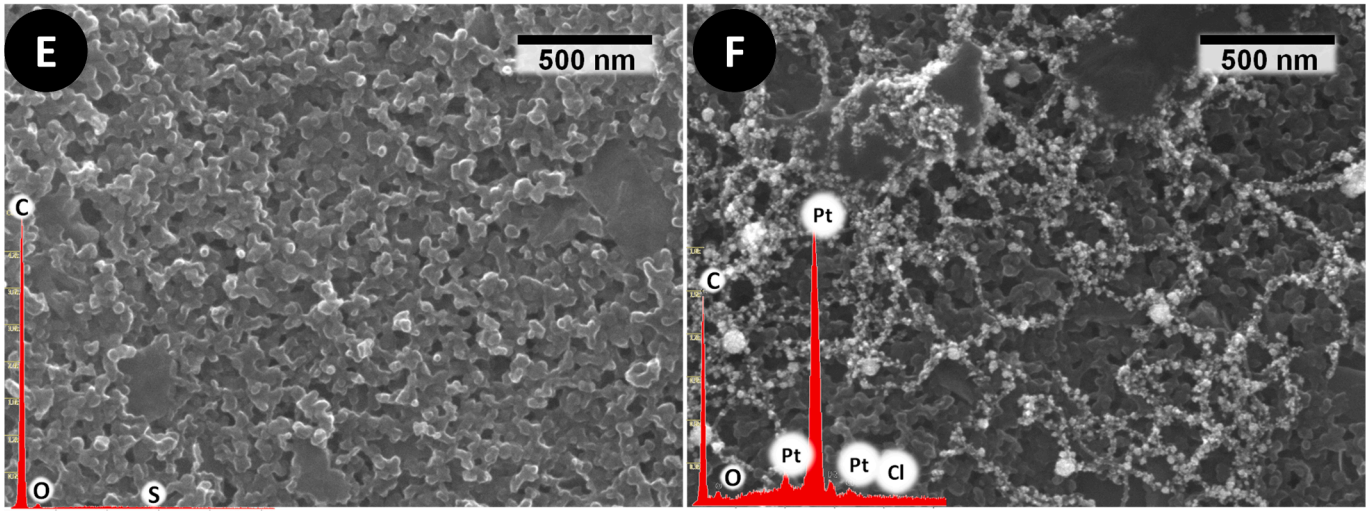

Fig. 2. A) CV and B) EIS response for bare C-SPE and treated C-SPE with sulphuric acid solution; C) Illustration of fabrication of MWCNTs-PAH/Pt-C-SPE; D) CV measurements before and after nanocomposite functionalization (at different temperatures); SEM images with EDS analysis of (E) treated C-SPE and (F) MWCNTs-PAH/Pt-C-SPE.

displayed a distinct pair of well-defined redox peaks, indicative of the reversible electron transfer of the $[Fe(CN)_6]^{3-/4-}$, enabling higher values of current after the cleaning protocol. Regarding the EIS results, charge transfer resistance (Rct) values were calculated by iterative fitting (software NOVA 2.1.4) of the experimental data to the Randle's equivalent circuit. Briefly, the solution resistance (Rs) and Rct values are determined in the high-frequency region, whereas the linear portion at lower frequencies corresponds to the impedance characterized by Warburg (Zw). This aspect is associated with the mass transfer of the redox species on the electrode surface, representing a diffusion process [44]. The obtained results showed that cleaned C-SPEs presented lower potential difference between oxidation and reduction peaks (ΔE_p) and smaller Rct values which is a strong indication of surface cleanliness.

Afterwards, the adsorption of the nanocomposite material on the previously treated C-SPE was tested at two different temperatures, 60 °C and 75 °C, for the 3 layers of material applied during 30 min of incubation each (Fig. 2C). Like expected, the voltammograms obtained after the immobilization of MWCNTs-PAH/Pt on C-SPE displayed an increase in both oxidation and reduction peak current intensities which is correlated to the better conductivity properties of the CNTs-Pt nanomaterials, as well as, to a higher surface area available (Fig. 2D). Although both tested conditions enabled greater electrochemical performance, a slightly higher response was observed with a 60 °C temperature of incubation, which was selected for subsequent work. This improved response can be attributed to enhanced temperature-dependent mechanisms, as a result of a more uniform and stable PAH conformation on the composite material. This effect is facilitated by i) conformational changes in the polymer chains, ii) improved amino group interactions, iii) optimized electrostatic forces, and iv) enhanced wetting and dispersion properties. These temperature-induced mechanisms collectively contribute to a more thermodynamically and kinetically favourable configuration of the composite material on the carbon surface, leading to higher electrochemical performance.

In parallel, SEM analysis was employed to characterize the morphology and distribution of the as-prepared nanomaterials onto the carbon electrode. Fig. 2E and F illustrate the surface images of the C-SPEs electrodes before and after MWCNTs-PAH/Pt functionalization, respectively. One can see that in the case of the cleaned electrode the surface presents a relative homogenous appearance, while after the deposition of the nanocomposite, a nanoparticle-web distribution can be observed attached to the surface, which are connected with each other, forming a three-dimensional structure with many pores. Furthermore, EDS analysis was used to provide an elemental composition of the observed areas and, characteristic elements like Pt, C, Cl and O could be observed, implying the successful adsorption of the MWCNTs-PAH/Pt material on the surface of C-SPEs.

3.2. Cyclodextrin-protein interaction

Looking back through some of the main issues addressed during the imprinting process of proteins, we can for sure find the important role of affinity interactions between the template and the monomer(s). In case

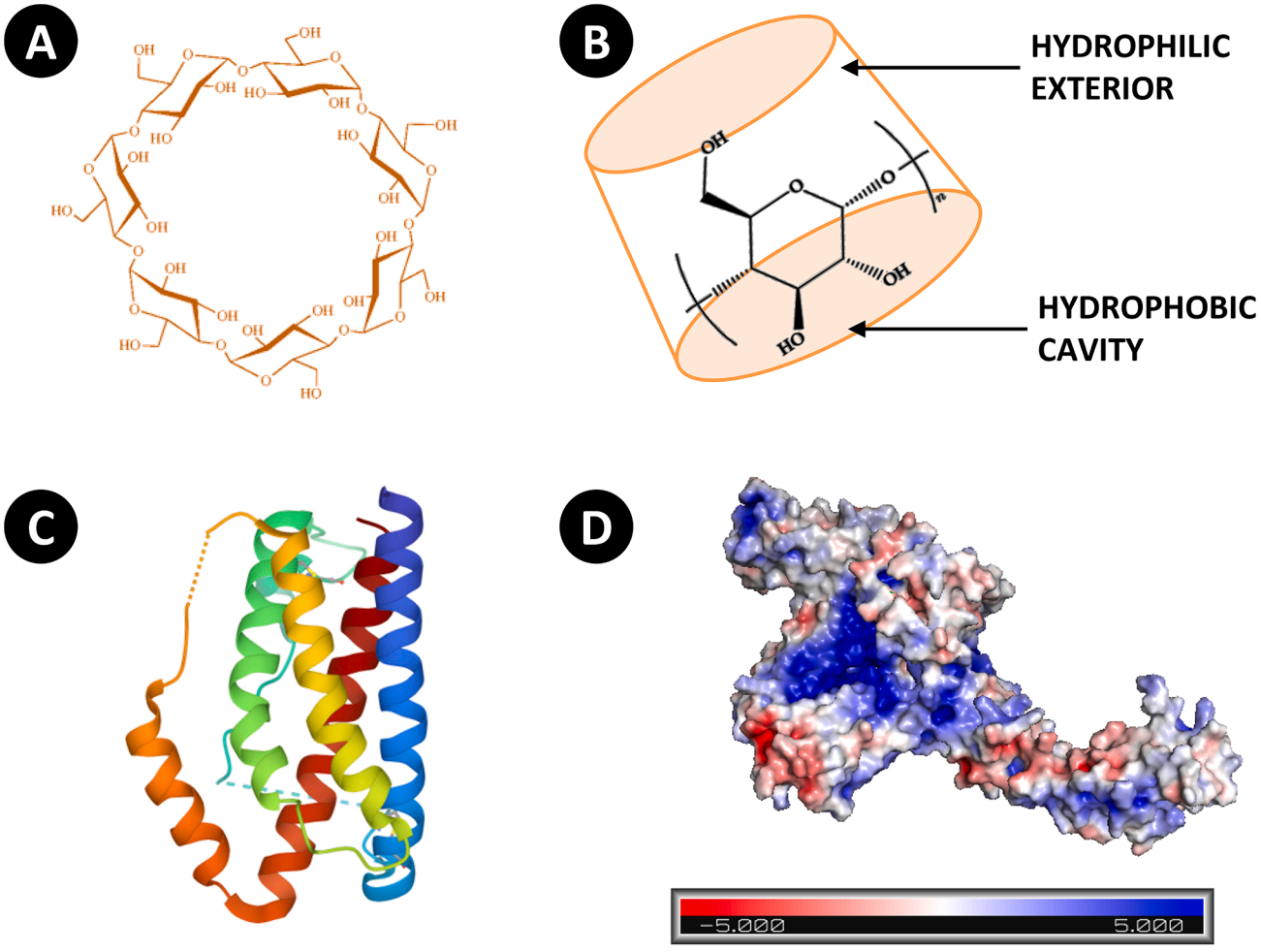

Fig. 3. A) Chemical structure and B) conventional representation (toroidal shape) of β-CD; C) Ribbon representation of the IL-6 protein structure (from Protein Data Bank); D) Electrostatic potential representation at a computed surface for the Human IL-6 (PDB file) at a pH of 5.0; The colour range corresponds to the predicted surface potential, where red indicates negativity, white represents neutrality, and blue signifies positivity. This range spans from −5.0 to +5.0. (kb T ec-1).

of these complex biomolecules, extra careful is required during the imprinting stage in order to prevent the alteration of the 3D folded structure of proteins, which can occur due to extreme pH and/or temperature conditions, removal of water and exposure to non-aqueous solvents [45]. In this context, CDs hold the ability to form complexes with different types of biomolecules like lipids, carbohydrates, proteins and nucleic acids [46]. Due to their peculiar structure, CDs are hydrophobic inside and hydrophilic outside, which gives them the opportunity to attract and accommodate hydrophobic moieties in the cavity (Fig. 3A and B). For this reason, computational studies and bulk simulations have illustrated the important role of β-CDs in the modulation and stabilization of conformational changes of proteins [47]. Moreover, previous investigations have been conducted with a model insulin protein and β-CD and the obtained results demonstrated that this interaction takes place at specific exposed sites on the protein surface, being highly dependent of the solvent accessibility conditions [48]. Overall, in solution conditions, the formation of inclusion complexes will be mainly driven by host-guest and electrostatic interactions [49] and for a given protein, the effect of CDs attraction and interaction will always be given by the particular structure of the protein.

From the point-of-view of biosensing, understanding the structure of IL-6 target protein is herein highly relevant as its intrinsic properties like molecule size and isoelectric point (pI) will directly influence the detection performance. Briefly, full-length IL-6 molecule is within the range of 21 to 28 kDa (Fig. 3C) comprised of 212 amino acids. It features an N-terminal signal peptide and a four-helix bundle organized in an up-up-down-down topology. This arrangement plays a crucial role in guiding IL-6 towards its appropriate orientation during receptor binding [50,51]. Regarding the pI of proteins, including IL-6, further examination of structural and charge alterations can give valuable information of the binding affinity between the protein template and the monomeric species. As the pI of IL-6 is predicted to be 6.24 (obtained from "IL-6 Compute pI/Mw," 2023), meaning that the protein will have a net positive charge in acidic conditions, a net negative charge in basic conditions and no net charge at its pI value. The 3D structure of human IL-6, a 185 amino acid polypeptide, was extracted from the Protein Data Bank (PDB) with the code 1alu. The PDB files were employed to visualize the distribution of surface charges, further enhancing our understanding of the protein's structure and the potential interactions with β-CD. According to Fig. 3D, it is possible to verify that the central region and part of the globular ends are the most electropositive parts of this protein, being strong candidates for hydrogen bond interaction between IL and 6 and the hydroxyl groups (hydrophilic rim) of β-CD. We believe that this information agrees with other biocompound studies where molecular docking results showed the formation of stable inclusion CD-complexes between guest and host in the presence of hydrogen bond interaction [52]. Besides, due to the hydrophobic parts of IL-6 protein, the inner hydrophobic pocket of β-CD provides a more stable and native complex matrix to attract the target molecule and to facilitate its absorption onto the electrode surface. Furthermore, molecular docking was carried out using AutoDock and AutoDockTools, employing rapid grid-based energy evaluation to predict small molecule binding modes and affinities with protein receptors. Fig. S1A illustrates the initial state with the ligand (β-CD) positioned at a distance from the protein (IL-6) before docking. The centered grid denotes the designated region for upcoming docking. In Fig. S1B, the first pose (*Mode 1*) among the nine generated indicates a high probability of binding on the pocket side. With a binding score of −9.7 kcal/mol, this optimal configuration confirms the successful performance of the molecular docking interaction between the IL-6 and β-CD.

3.3. Fabrication and follow-up of the biosensing platform

Alongside with the aforementioned properties that make nanomaterials so attractive for surface functionalization, herein the immobilization of MWCNTs-PAH/Pt material also enables the introduction of amine groups directly on the carbon electrode surface. Thus, without affecting any activity and structure of the biocomponent, the incorporation of these functional groups on the electrical platform can promote a better adhesion of the subsequent layers and encourage a more controlled growth of the electropolymerizable film that, ultimately, results in a reproducibility enhancement. Initially, electrochemical assays were conducted to better understand the voltametric behaviour of β-CD electropolymerized on the modified C-SPE surface. As shown in Fig. 4A, the electropolymerization was performed by first scanning the potential between −1.0 V and +1.3 V, at 100 mV/s, during 20 successive cycles. Although it was observed an increase of the peak current (at −0.6 V) with an increment of CV cycles, meaning that the formed polymeric film displays a typical conductive behavior [53], the inset EIS data confirmed that the polymeric material was not successfully attached to the functionalized carbon platform. Furthermore, a slight oxidation peak is visible around +0.6 V that was ascribed to the production of β-CD cationic radicals [17]. Nevertheless, no significant differences were observed regarding the Rct values measured after applying the potential range with buffer solution alone and in the presence of β-CD monomer. This outcome can be explained due to the need of high energy that can be achieved with a wider range of potential applied during the electrochemical polymerization. This type of difficulties during the polymerization process of β-CD-containing systems has already been reported in literature [54]. So, to overcome this limitation and continue to operate at mild conditions, herein it was used a mixture of Py with β-CD as the monomer solution to electrochemically growth the biomimetic polymer material. SCP like Py have been widely applied in the design of catalytic and affinity biosensors due to their unique capability to transfer electrical charge resulting in the amplification of analytical signal [55]. Fig. 4B shows the cyclic voltammograms of a mixture containing β-CD (1 mM) and Py (2.5 mM) prepared in 0.15 mol/L phosphate-citrate buffer at pH 5.0 on the modified C-SPE. The electropolymerization was performed by applying 30 consecutive voltametric cycles between 0 V and +1.8 V at a scan rate of 100 mV/s. It was observed a broad peak at about +0.9 V for the NIP modified electrode that was attributed to Py oxidation, which is a similar result to other previous studies [24]. Moreover, with an increase in the number of cycles, the current intensity exhibited a gradual decrease, indicating the formation and deposition of a non-conductive NIP film onto the modified C-SPE surface.

To accomplish a sensitive poly(β-CD-Py) polymeric film, to be used as an electrochemical sensor, some relevant parameters need to be carefully optimized, such as, monomers and protein concentrations. Since β-CD was incorporated in this MIP design in order to exploit its host-guest inclusion property and, consequently, contain the target protein, a concentration of 1 mM was fixed. Meanwhile, 3 different concentrations of Py on the monomer mixture were tested, as illustrated in Fig. 4C. Looking to the EIS data, it was clear that an increment of the Rct value was obtained with increasing Py monomer concentrations $1<2.5<5$ mM, which comprises the passivating nature of the polymeric layer formed on the transducer surface. Thus, 2.5 mM was selected as the optimum Py concentration because a higher value can hinder the sensitivity of the sensing device and, on the other hand, the lower concentration was characterized by a quite subtle variation on the Rct value, meaning that the stability of the polymeric film can be compromised. Another crucial factor that significantly influences the response of the biosensor concerns the concentration and distribution of the recognition sites available on the surface of the imprinted material [56,57]. Thus, the concentration of IL-6 in the polymerization mixture was also investigated in this work. For this purpose, MIP films were electrochemically synthesized by varying the concentration of the template protein between 4.78×10^{-8} M (1.0 μg/mL) e 4.78×10^{-9} M (0.1 μg/mL). Fig. 4D presents the Nyquist diagrams of NIP and MIP electrodes fabricated at similar conditions, with the exception of the protein concentration (0, 0.1 and 1.0 μg/mL) during the polymerization reaction. The results revealed a significant impact due to the

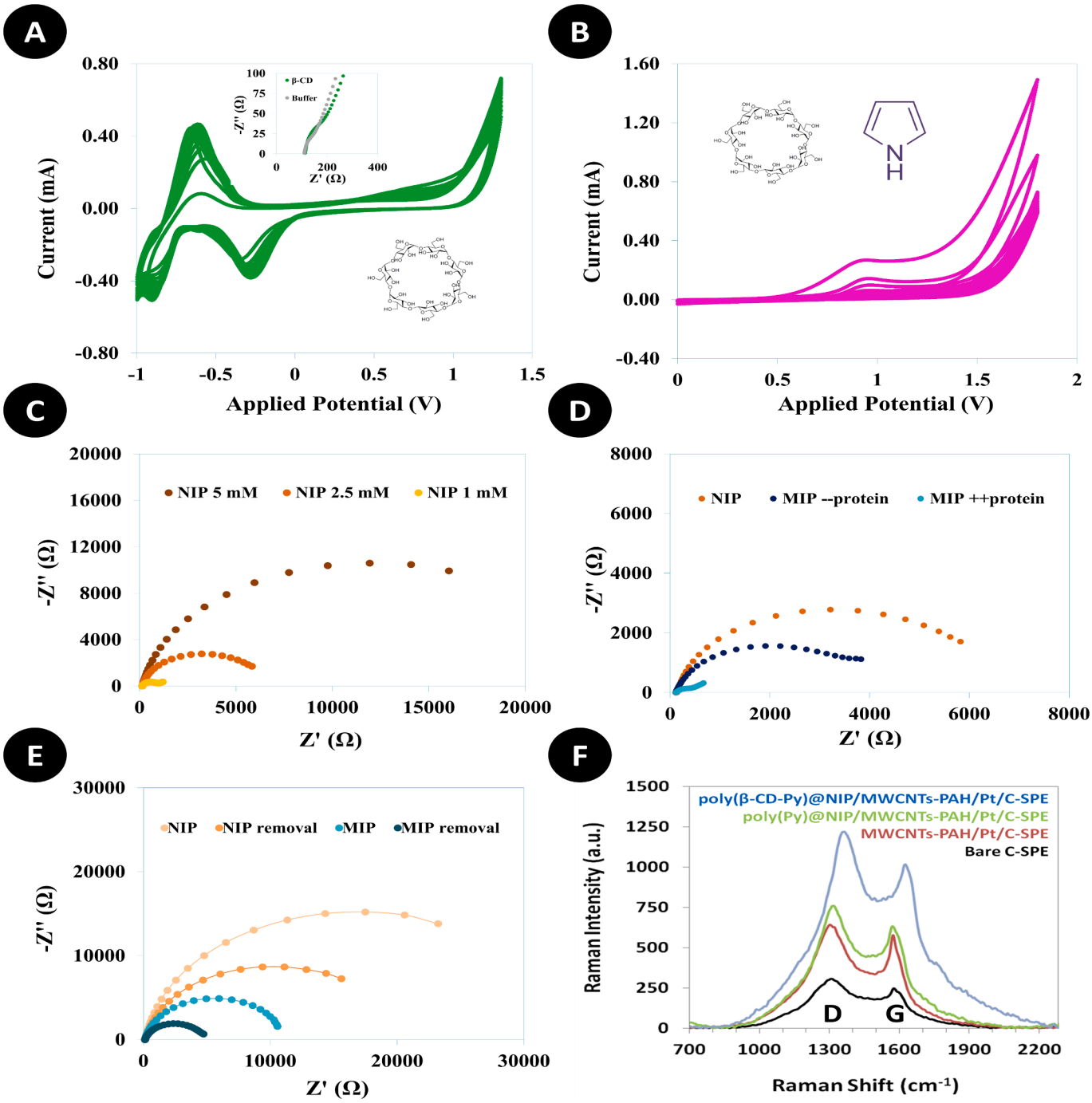

Fig. 4. Cyclic voltammograms regarding electropolymerization of A) β-CD monomer and B) a mixture containing β-CD and pyrrole monomers, at modified C-SPE. EIS data obtained during the optimization studies of the electrochemical polymerization of C) NIPs with different concentrations of pyrrole monomer (1, 2.5 and 5 mM) and D) MIPs with different concentrations of IL-6 protein (0.1 and 1 μg/mL). E) EIS measurements of NIP and MIP electrodes, before and after the removal step. F) Raman spectra of the modified electrodes after each modification: bare C-SPE (black line); functionalized electrode MWCNTs-PAH/Pt-C-SPE (red line); non-imprinted material after polymerization with pyrrole alone, poly(Py)@NIP/MWCNTs-PAH/Pt-C-SPE (green line) and with both β-CD and pyrrole monomers, poly(β-CD-Py) @NIP/MWCNTs-PAH/Pt-C-SPE (blue line).

incorporation of the protein within the polymeric matrix, leading to a considerable decrease of Rct, which can be explained based on the diffusional behaviour of the redox pair $[Fe(CN)_6]^{3-/4-}$ marker through the porous MIP film. Like mentioned before, IL-6 protein is a non-electroactive compound with a pI of 6.24, meaning that at a pH of 5.0 the charge distribution of the protein is predominantly positive. So, for higher concentrations of IL-6 protein entrapped during the electro-polymerization event, the MIP sensor surface will become positively charged and consequently, the negative redox couple ions will be attracted to electrode-electrolyte interface, causing a substantial decrease of the Rct observed. Moreover, the presence of this biomolecule of high molecular weight in the carbon surface of the electrode can also hinder in some way the polymerization reaction [58,59]. So, looking into the impedimetric data, the lower concentration of IL-6 (0.1 μg/mL) was selected as the optimum template concentration for the subsequent assays.

The final step in the fabrication process of the MIP sensor concerns the removal of the entrapped protein. This constitutes a critical stage for

Table 1
Analytical information obtained from Raman spectra related to various modifications.

Sample	D position (cm^{-1})	I(D)	G position (cm^{-1})	I(G)	I_D/I_G
Bare C-SPE	1311.14	316.680	1576.68	259.575	1.22
MWCNTs-PAH/Pt-C-SPE	1302.23	656.730	1572.89	591.142	1.11
poly(Py)@NIP/MWCNTs-PAH/Pt-C-SPE	1318.60	878.810	1570.57	756.220	1.16
poly(β-CD-Py)@NIP/MWCNTs-PAH/Pt-C-SPE	1318.52	1287.462	1580.61	1082.657	1.19

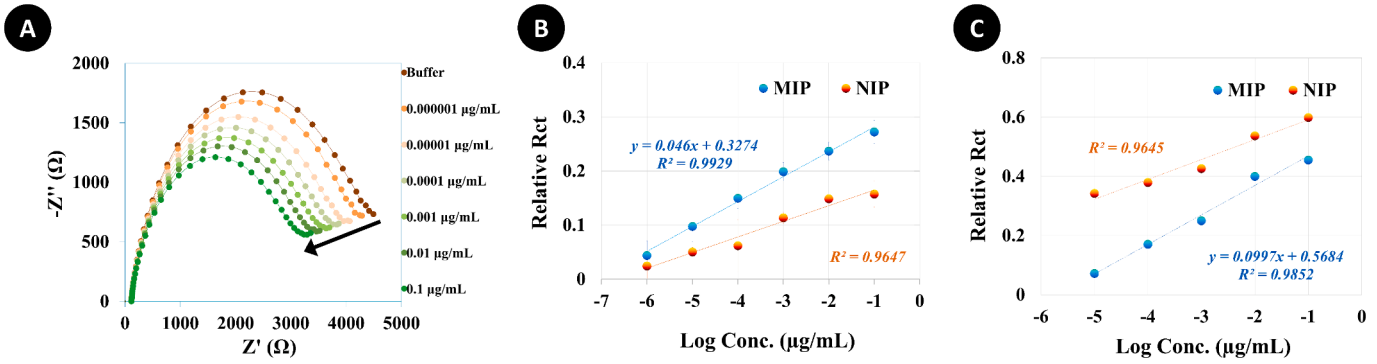

Fig. 5. A) Nyquist plot of MIP sensor, previously incubated in increasing concentrations of IL-6. Calibration curves regarding the electrochemical response change by EIS for MIP and NIP electrodes toward IL-6 concentration in B) phosphate-citrate buffer solution and C) diluted human serum solution.

Table 2
Some examples of electrochemical biosensors for IL-6 detection.

Biorecognition Element	Electrochemical Detection	Linear Detection Range	Limit of Detection	Reference
Antibody	CV	0.006–0.020 ng/mL	0.005 ng/mL	[74]
Antibody	Amperometry	4.0–8.0×10^2 pg/mL	1.0 pg/mL	[40]
Antibody	SWV	10^{-3}-10^3 ng/mL	0.1 pg/mL	[39]
Antibody	EIS	0.003–75 ng/mL	1 pg/mL	[68]
Antibody	DPV	10–500 pg/mL	5.1 pg/mL	[69]
Antibody	SWV	26–125 and 30–138 pg/mL	4.8 pg/mL	[41]
Aptamer	EIS	1 pg/mL – 15 μg/mL	0.33 pg/mL	[71]
MIP	EIS	0.02 pg/mL – 20 ng/mL	0.02 pg/mL	[61]
MIP	DPV	0.01–2.0 pg/mL	0.0030 pg/mL	[72]
MIP	EIS	1–200 pg/mL	0.25 pg/mL	[75]
MIP	EIS	1 pg/mL – 100 ng/mL	1 pg/mL	*This work*

CV: cyclic voltammetry; DPV: differential pulse voltammetry; EIS: electrochemical impedance spectroscopy; MIP: molecularly imprinted polymer; SWV: square wave voltammetry.

the MIP sensor performance and can be highly difficult by the high size and complex nature of protein biomolecules. Among the most common and popular methods used for this purpose we can find enzymatic and acidic approaches [60–63]. Therefore, herein both approaches, incubation in proteinase k and in oxalic acid solutions, were tested alone and in combination. In all the employed removal protocols it was included a final incubation step in buffer solution in order to stabilize the charges as a consequence of the pH variations. Fig. 4E illustrates the Nyquist diagrams for NIP and MIP electrodes before and after an oxalic acidic treatment, that was the selected removal approach since it enabled higher variations. As can be seen, after incubation in acidic solution it was observed a substantial decrease of the Rct value of the MIP biosensor, suggesting that IL-6 was successfully extracted from the polymer. This could be attributed to the elution of the template molecules from the MIP film and, therefore, the compact surface of the modified electrode becomes looser and more porous, facilitating the electron transfer on the surface of the electrode. Although the control experiments, performed on the film polymerized in the absence of IL-6 (NIP), also presented a visible variation this can be explained due to protonation variations that are occurring on the polymeric backbone that also affect its conductivity behaviour [64].

At each stage of the biosensor assembly's chemical modification, the carbon surface was subjected to characterization through Raman spectroscopy. This powerful tool is commonly used for studying disorder and defects in crystal structure especially for carbon-based materials [65,66]. Like displayed in Fig. 4F, the obtained spectra present the typically so-called G- and D-bands, lying at around 1570 and 1310 cm^{-1}, respectively [67]. Both bands correspond to sp^2 sites, more specifically, the G-band arises from the bond stretching of all pairs of sp^2 atoms while the D-bands are linked to the so-called breathing modes of sp^2 atoms in rings [67]. To characterize the structural disorder of the carbon material, the ratio of intensities of the aforementioned bands (ID/IG) was analysed. Table 1 shows the peak positions of the G and D bands in the different modified materials, as well as the corresponding intensities. While the ID/IG ratios exhibited a consistent trend across the different electrodes, it was interesting to note that after the incorporation of the nanomaterial into the carbon surface, the ID/IG value decreased from 1.22 to 1.11 which constitutes a strong indication that the modification of C-SPE provides a more organized carbon structure (less disorder). Furthermore, the inclusion of this type of nanomaterial also yielded changes in the Raman shift of the D peak position, shifting to lower values, 1302.23 cm^{-1}. As expected, the addition of a non-imprinted polymeric layer on the modified C-SPE contributed to disorder of the sp^2 carbon system, leading to higher ID/IG ratio. The NIP containing both β-CD and Py monomers showed the higher ratio and consequently, an increase of the defects in the structure possibly due to the formation of a more polymeric material.

3.4. Response of the MIP biosensor

Under the optimized experimental conditions, the analytical performance of IL-6 sensing material was evaluated by recording calibration curves in buffer solution, as shown in Fig. 5A. EIS calibration curves were plotted with the Rct of MIP and corresponding NIP against the logarithm concentration of IL-6 (Fig. 5B). Our results showed that the Rct value of the MIP sensor decreased in the presence of IL-6 protein which constitutes an indication of a quicker charge transfer and improved electrochemical conductivity. Although the most usual response observed after protein binding is an increasing effect of Rct due to blocking redox probe access to the electrode surface, herein the isoelectric point of IL-6 must be considered to understand the obtained opposite effect. If we look to the environmental surrounding conditions, the buffer solution holds a pH of 5.0 and consequently, the IL-6 protein is predominantly positively charged due to its pI value. After the arrival of the protein at the cavity local sites, the access is blocked by its presence but, simultaneously, the surface charge becomes more positive due to IL-6 presence and the negatively charged redox pair can be attracted to the electrode surface, enabling a faster charge transfer. The calibration curve obtained for the MIP sensor showed a logarithmic relationship over the IL-6 concentration range [1 pg/ml – 100 ng/mL]. Each concentration was subjected to three independent measurements. In parallel, the response of the control electrode (NIP) was also assessed, and it was also observed a variation of the Rct but a very poor linear correlation (r^2 – 0.96), with an inferior slope.

Another important requirement is that MIPs must have specific selectivity towards the template molecule. With the purpose to evaluate MIP selectivity, the electrochemical detection of IL-6 was also performed in a human serum matrix (1:100 diluted in phosphate-citrate buffer). Briefly, the complex matrix solution was spiked with different amounts of standard IL-6 solution and then, a calibration curve was constructed (Fig. 5C). Our results showed that the MIP material enabled the selective quantification of IL-6 from 10 pg/ml to 100 ng/mL, showing a good linear correlation. In contrast, the NIP electrode presented a poor linear correlation (r^2 ~0.96) which could be assigned to non-specific binding of the protein molecules.

So far, different types of electrochemical sensors for IL-6 detection have been functionalized using different biorecognition elements like antibodies, aptamers, MIPs, among others (see Table 2). Currently, antibodies continue to be the most used capture technique in the design of biosensors towards IL-6 monitoring as a result of their high specificity [68–70]. Nevertheless, these natural elements are costly and quite vulnerable to degradation. Aiming for improved stability and with longer shelf life than antibodies, aptamers appear as single strands of DNA or RNA that fold into three-dimensional structures and possess the capability to selectively bind to antigens such as IL-6 [71]. However, aptamers may exhibit limitations such as susceptibility to nuclease degradation and potential off-target binding. Like aptamers, MIPs are cost-effective, easy to synthesize and more durable in harsh environmental conditions than the natural-based approaches. If we look through the literature in the last years, very few electrochemical MIP sensors can be found for IL-6 detection in complex biological matrices [61,72,73]. Thus, the proposed biosensor presents suitable sensitivity and selectivity characteristics to be applied for IL-6 ultratrace analysis, down to picogram level, in human serum samples.

Regarding its biological levels, after production, IL-6 is released in the bloodstream to communicate with the surrounding body tissues. Consequently, biofluids, such as, serum, blood and plasma are highly valuable to be used for IL-6 detection. As an example, a study has been conducted on patients with a myocardial infarction, where plasma IL-6 levels were 46.5±7.8 pg/mL against healthy levels of 6.7±1.2 pg/mL [73]. Also, elevated levels of IL-6 in cerebrospinal fluid and serum of Alzheimer patients have been considered a significant contributor to neuroinflammation events [76]. Moreover, the aging populations have presented an elevated prevalence of chronic inflammation that, in most cases, is accompanied by an increased systemic concentration of IL-6 in biological fluids [77]. Overall, our findings have showcased the potential of this imprinted-modified sensor to be used as a potential monitoring tool for sensitively quantify IL-6 in complex biological matrices.

4. Conclusions

The here presented MIP sensor targeting IL-6 protein has been carefully optimized and characterized, resulting in a good analytical performance evaluated both in buffer solution and in diluted human serum. During the electropolymerization, the optimization of experimental parameters like potential range applied, ratio protein-monomers and template removal approach were vital for successful imprinting. In parallel, the authors also demonstrated that the combination of hydrophobic effect and electrostatic interaction between the natural-based system β-CD and IL-6 protein during the molecular imprinting process can constitute a great improvement in terms of selectivity and sensitivity features. The fabricated poly(β-CD-Py)@MIP/MWCNTs-PAH/Pt-C-SPE biosensor was used for the quantitative analysis of the IL-6 biomarker over the concentration range 1 pg/ml to 100 ng/mL. Thus, the use of binary functional monomers can be a feasible pathway for achieving superior molecular recognition in aqueous media. Furthermore, the direct adsorption of a highly catalytic nanomaterial with a rather simple one-step procedure for the electrochemical MIP manufacturing process make this a promising sensing device to be used for cytokine monitorization.

CRediT authorship contribution statement

Bianca Ferreira: Writing – review & editing, Methodology. **Miguel Correa-Duarte:** Writing – review & editing, Investigation. **Arcelina Marques:** Writing – review & editing, Investigation. **Felismina Moreira:** Writing – review & editing, Investigation, Conceptualization. **Gabriela Martins:** Conceptualization, Supervision, Validation, Writing – review & editing.

Declaration of competing interest

The authors declare that they have no known competing financial interests or personal relationships that could have appeared to influence the work reported in this paper.

Data availability

The authors are unable or have chosen not to specify which data has been used.

Acknowledgments

The authors acknowledge funding to the Portuguese Foundation for Science and Technology (FCT) through the project SmartBioPatch (EXPL/CTM-REF/1095/2021) and through the grants UIDB/04730/2020 and UIDP/04730/2020.

Appendix A. Supplementary data

Supplementary data to this article can be found online at https://doi.org/10.1016/j.microc.2024.110345.

References

[1] J. Wackerlig, P.A. Lieberzeit, Molecularly imprinted polymer nanoparticles in chemical sensing - synthesis, characterisation and application, Sens Actuators B Chem. 207 (2015) 144–157.
[2] L. Chen, X. Wang, W. Lu, X. Wu, J. Li, Molecular imprinting: perspectives and applications, Chem. Soc. Rev. 45 (2016) 2137–2211.

[3] Y. Saylan, A. Denizli, Molecularly imprinted polymer-based microfluidic systems for point-of-care applications, Micromachines (basel). 10 (2019) 1–14.
[4] B. Tse Sum Bui, T. Auroy, K. Haupt, Fighting antibiotic-resistant bacteria : promising strategies orchestrated by Molecularly imprinted Polymers, Angew Chem Int Ed Engl. 14 (2022) 1–18.
[5] M.M. Ali, S. Zhu, F.R. Amin, D. Hussain, Z. Du, L. Hu, Molecular imprinting of glycoproteins: from preparation to cancer theranostics, Theranostics. 12 (2022) 2406–2426.
[6] P. Sergey, T. Anthony, Molecular imprinting of Polymers, 1st ed., CRC Press, 2006.
[7] M.F. Frasco, L.A.A.N.A. Truta, M.G.F. Sales, F.T.C. Moreira, Imprinting Technology in Electrochemical Biomimetic Sensors, Sensors. 17 (2017) 1–29.
[8] O.I. Parisi, F. Francomano, M. Dattilo, F. Patitucci, S. Prete, F. Amone, F. Puoci, The evolution of Molecular recognition : from antibodies to Molecularly imprinted Polymers (MIPs) as artificial Counterpart, J Funct Biomater. 13 (2022) 1–26.
[9] G. Yang, F. Zhao, Electrochemical sensor for chloramphenicol based on novel multiwalled carbon nanotubes@molecularly imprinted polymer, Biosens Bioelectron. 64 (2015) 416–422.
[10] A.R. Cardoso, A.P.M. Tavares, M.G.F. Sales, In-situ generated molecularly imprinted material for chloramphenicol electrochemical sensing in waters down to the nanomolar level, Sens Actuators B Chem. 256 (2018) 420–428.
[11] K. Parate, C. Karunakaran, J.C. Claussen. Electrochemical cotinine sensing with a molecularly imprinted polymer on a graphene-platinum nanoparticle modi fi ed carbon electrode towards cigarette smoke exposure monitoring. Sens Actuators B Chem. 287. (2019). 165–172.
[12] G. Crini, Review: a history of cyclodextrins, Chem Rev. 114 (2014) 10940–10975.
[13] J. Wankar, N.G. Kotla, S. Gera, S. Rasala, A. Pandit, Y.A. Rochev, Recent advances in host-guest self-assembled cyclodextrin Carriers: implications for responsive drug delivery and biomedical engineering, Adv Funct Mater. 30 (2020) 1909049.
[14] G. Yu, X. Chen, Host–guest chemistry in supramolecular theranostics, Theranostics. 9 (2019) 3041–3074.
[15] A. Zarepour, A. Zarrabi, K.L. Larsen, Fabricating B-cyclodextrin based pH-responsive nanotheranostics as a programmable polymeric nanocapsule for simultaneous diagnosis and therapy, Int J Nanomedicine. 14 (2019) 7017–7038.
[16] Z. Liu, Q. Wang, Q. Xue, C. Chang, R. Wang, Y. Liu, Highly efficient detection of ofloxacin in water by samarium oxide and β-cyclodextrin-modified laser-induced graphene electrode, Microchemical Journal. 186 (2023) 108353.
[17] Q. Qin, X. Bai, Z. Hua, Electropolymerization of a conductive β-cyclodextrin polymer on reduced graphene oxide modified screen-printed electrode for simultaneous determination of ascorbic acid, dopamine and uric acid, Journal of Electroanalytical Chemistry. 782 (2016) 50–58.
[18] F. Zhang, S. Gu, Y. Ding, Z. Zhang, L. Li, A novel sensor based on electropolymerization of β-cyclodextrin and l-arginine on carbon paste electrode for determination of fluoroquinolones, Anal Chim Acta. 770 (2013) 53–61.
[19] M. Wei, X. Geng, Y. Liu, H. Long, J. Du, A novel electrochemical sensor based on electropolymerized molecularly imprinted polymer for determination of luteolin, Journal of Electroanalytical Chemistry. 842 (2019) 184–192.
[20] Z. Jiang, G. Li, M. Zhang, Electrochemical sensor based on electro-polymerization of β-cyclodextrin and reduced-graphene oxide on glassy carbon electrode for determination of gatifloxacin, Sens Actuators B Chem. 228 (2016) 59–65.
[21] A. Bolognesi, M.C. Pasini, Semiconducting Polymers: chemistry, physics and engineering, 2nd ed., WILEY-VCH, 2007.
[22] Á. Terán-Alcocer, F. Bravo-Plascencia, C. Cevallos-Morillo, A. Palma-Cando, Electrochemical sensors based on conducting polymers for the aqueous detection of biologically relevant molecules, Nanomaterials. 11 (2021) 1–62.
[23] J. Xu, Y. Zhang, K. Wu, L. Zhang, S. Ge, J. Yu, A molecularly imprinted polypyrrole for ultrasensitive voltammetric determination of glyphosate, Microchimica Acta. 184 (2017) 1959–1967.
[24] E. Mathieu-Scheers, S. Bouden, C. Grillot, J. Nicolle, F. Warmont, V. Bertagna, B. Cagnon, C. Vautrin-Ul, Trace anthracene electrochemical detection based on electropolymerized-molecularly imprinted polypyrrole modified glassy carbon electrode, Journal of Electroanalytical Chemistry. 848 (2019) 113253.
[25] X. Kan, Z. Xing, A. Zhu, Z. Zhao, G. Xu, C. Li, H. Zhou, Molecularly imprinted polymers based electrochemical sensor for bovine hemoglobin recognition, Sens Actuators B Chem. 168 (2012) 395–401.
[26] M. Garg, N. Vishwakarma, B. Mizaikoff, S. Singh, Molecularly imprinted conducting Polymer based sensor for Salmonella typhimurium detection, Bioelectrochemistry. 147 (2022) 108211.
[27] N. Ermiş, N. Tinkiliç, Preparation of molecularly imprinted polypyrrole modified gold electrode for determination of tyrosine in biological samples, Int J Electrochem Sci. 13 (2018) 2286–2298.
[28] D. Işık, S. Şahin, M.O. Caglayan, Z. Üstündağ, Electrochemical impedimetric detection of kanamycin using molecular imprinting for food safety, Microchemical Journal. 160 (2020) 105713.
[29] J.F. Rusling, G.W. Bishop, N.M. Doan, F. Papadimitrakopoulos, Nanomaterials and biomaterials in electrochemical arrays for protein detection, J. Mater. Chem. b. 2 (2014) 12–30.
[30] M. Medina-Sánchez, S. Miserere, A. Merkoçi, Nanomaterials and lab-on-a-chip technologies, Lab Chip. 12 (2012) 1932.
[31] A. Zamora-Gálvez, E. Morales-Narváez, C.C. Mayorga-Martinez, A. Merkoçi, Nanomaterials connected to antibodies and molecularly imprinted polymers as bio/receptors for bio/sensor applications, Appl Mater Today. 9 (2017) 387–401.
[32] M. Pan, L. Hong, X. Xie, K. Liu, J. Yang, S. Wang, Nanomaterials-based Surface protein imprinted Polymers: synthesis and medical applications, macromol, Chem Phys. 222 (2021) 1–18.
[33] G. Ramesh, A.G. Maclean, M.T. Philipp, Cytokines and chemokines at the crossroads of neuroinflammation, neurodegeneration, and neuropathic pain, Mediators Inflamm. 2013 (2013) 480739.
[34] T. Kishimoto, The biology of interleukin-6, Blood 74 (1989) 1–10.
[35] R.F. Frye, V.M. Schneider, C.S. Frye, A.M. Feldman, Plasma levels of TNF-α and IL-6 are inversely related to cytochrome P450-dependent drug metabolism in patients with congestive heart failure, J Card Fail. 8 (2002) 315–319.
[36] Y. Liu, H. Qing, Y. Deng, Biomarkers in Alzheimer's disease analysis by mass spectrometry-based proteomics, Int J Mol Sci. 15 (2014) 7865–7882.
[37] H. Kalish, T.M. Phillips, Application of immunoaffinity capillary electrophoresis to the measurements of secreted cytokines by cultured astrocytes, J Sep Sci. 32 (2009) 1605–1612.
[38] S. Rink, B. Kaiser, M.S. Steiner, A. Duerkop, A.J. Baeumner, Highly sensitive interleukin 6 detection by employing commercially ready liposomes in an LFA format, Anal Bioanal Chem. 414 (2022) 3231–3241.
[39] J.J. Shi, T.T. He, F. Jiang, E.S. Abdel-Halim, J.J. Zhu, Ultrasensitive multi-analyte electrochemical immunoassay based on GNR-modified heated screen-printed carbon electrodes and PS@PDA-metal labels for rapid detection of MMP-9 and IL-6, Biosens Bioelectron. 55 (2014) 51–56.
[40] G. Wang, H. Huang, G. Zhang, X. Zhang, B. Fang, L. Wang, Dual amplification strategy for the fabrication of highly sensitive interleukin-6 amperometric immunosensor based on poly-dopamine, Langmuir. 27 (2011) 1224–1231.
[41] R. Cancelliere, A. Di Tinno, A.M. Di Lellis, G. Contini, L. Micheli, E. Signori, Cost-effective and disposable label-free voltammetric immunosensor for sensitive detection of interleukin-6, Biosens Bioelectron. 213 (2022) 114467.
[42] M. Eduarda Schneider, L. Guillade, M.A. Correa-Duarte, F.T.C. Moreira, Development of a biosensor for phosphorylated tau 181 protein detection in Early-stage Alzheimer's disease, Bioelectrochemistry. 145 (2022) 108057.
[43] N.S. Shah, V. Thotathil, S.A. Zaidi, H. Sheikh, M. Mohamed, Picomolar or beyond limit of detection using Molecularly imprinted Polymer-based electrochemical sensors : a review, Biosensors (basel). 12 (2022) 1107.
[44] J. Muñoz, R. Montes, M. Baeza, Trends in electrochemical impedance spectroscopy involving nanocomposite transducers: characterization, architecture surface and bio-sensing trends in electrochemical impedance spectroscopy involving nanocomposite transducers: characte, Trends in Analytical Chemistry. 97 (2017) 201–215.
[45] N.W.a.C. Turner, C.W.b Jeans, K.R.b. Brain, C.J.b. Allender, V.c. Hlady, D.W.c. D. Britt, From 3D to 2D: a review of the molecular imprinting of proteins, Biotechnol Prog. 22 (2006) 1474–1489.
[46] L. Leclercq, Interactions between cyclodextrins and cellular components: Towards greener medical applications? Beilstein Journal of Organic Chemistry. 12 (2016) 2644–2662.
[47] M. Rospiccio, A. Arsiccio, G. Winter, R. Pisano, The role of cyclodextrins against Interface-induced denaturation in Pharmaceutical formulations: a Molecular dynamics approach, Mol Pharm. 18 (2021) 2322–2333.
[48] F.L. Aachmann, D.E. Otzen, K.L. Larsen, R. Wimmer, Structural background of cyclodextrin-protein interactions, Protein Eng. 16 (2003) 905–912.
[49] R. Challa, A. Ahuja, J. Ali, R.K. Khar, Cyclodextrins in drug delivery: an updated review, AAPS PharmSciTech. 6 (2005) 329–357.
[50] A.D. Gelinas, D.R. Davies, T.E. Edwards, J.C. Rohloff, J.D. Carter, C. Zhang, S. Gupta, Y. Ishikawa, M. Hirota, Y. Nakaishi, T.C. Jarvis, N. Janjic, Crystal structure of interleukin-6 in complex with a modified nucleic acid ligand, Journal of Biological Chemistry. 289 (2014) 8720–8734.
[51] E. Niculet, V. Chioncel, A. Elisei, M. Miulescu, O. Buzia, L. Nwabudike, M. Craescu, M. Draganescu, F. Bujoreanu, E. Marinescu, M. Arbune, D. Radaschin, C. Bobeica, A. Nechita, A. Tatu, Multifactorial expression of IL–6 with update on COVID–19 and the therapeutic strategies of its blockade (review), Exp Ther Med. 21 (2021) 1–10.
[52] H. Alrabiah, A. Homoda, A. Bakheit, G. Ae Mostafa, Cyclodextrin potentiometric sensors based on selective recognition sites for procainamide: Comparative and theoretical study, Open Chem. 17 (2019) 1222–1234.
[53] A.C. Pereira, A.E.F. Oliveira, G.B. Bettio, β-Cyclodextrin electropolymerization: mechanism, electrochemical behavior, and optimization, Chemical Papers. 73 (2019) 1795–1804.
[54] T.V. Shishkanova, N. Habanová, M. Řezanka, G. Broncová, P. Fitl, M. Vrňata, P. Matějka, Molecular recognition of phenylalanine Enantiomers onto a solid Surface modified with Electropolymerized pyrrole-β-cyclodextrin conjugate, Electroanalysis. 32 (2020) 767–774.
[55] K. Glosz, A. Stolarczyk, Electropolymerised polypyrroles as active layers for Molecularly imprinted sensors : fabrication and applications, Materials 14 (2021) 1369.
[56] H. Shekarchizadeh, A.A. Ensafi, M. Kadivar, Selective determination of sucrose based on electropolymerized molecularly imprinted polymer modified multiwall carbon nanotubes/glassy carbon electrode, Mater Sci Eng C Mater Biol Appl. 33 (2013) 3553–3561.
[57] H. Hrichi, L. Monser, N. Adhoum, Selective electrochemical determination of etoposide using a Molecularly imprinted overoxidized polypyrrole coated glassy Carbon electrode, International Journal of Electrochemistry. 2019 (2019) 1–12.
[58] G.V. Martins, A.C. Marques, E. Fortunato, M.G.F. Sales, Paper-based (bio)sensor for label-free detection of 3-nitrotyrosine in human urine samples using molecular imprinted polymer, Sens Biosensing Res. 28 (2020) 100333.
[59] Y. Yuan, T. Li, Z. Ye, Y. Feng, Z. Chen, Y. Wang, Y. Sun, H. Wu, Z. Yang, Y. Wang, Y. Zhang, L. Huang, B. Liang, A one-step Electropolymerized biomimetic polypyrrole membrane-based electrochemical sensor for selective detection of valproate, front bioeng, Biotechnol. 10 (2022) 1–8.

[60] S. Khumngern, P. Thavarungkul, P. Kanatharana, T. Bejrananda, A. Numnuam, Molecularly imprinted electrochemical sensor based on poly(o-phenylenediamine-co-o-aminophenol) incorporated with poly(styrenesulfonate) doped poly(3,4-ethylenedioxythiophene) ferrocene composite modified screen-printed carbon electrode for highly sensitive, Microchemical Journal. 177 (2022) 107311.
[61] M. de L. Gonçalves, L.A.N. Truta, M.G.F. Sales, F.T.C. Moreira, Electrochemical point-of Care (PoC) determination of Interleukin-6 (IL-6) using a pyrrole (py) Molecularly imprinted Polymer (MIP) on a Carbon-screen printed electrode (C-SPE), Anal Lett. (2021) 1–13.
[62] E. Komarova, M. Aldissi, A. Bogomolova, Design of molecularly imprinted conducting polymer protein-sensing films via substrate–dopant binding, Analyst. 140 (2015) 1099–1106.
[63] F.T.C. Moreira, S. Sharma, R.a.F. Dutra, J.P.C. Noronha, A.E.G. Cass, M.G.F. Sales, Smart plastic antibody material (SPAM) tailored on disposable screen printed electrodes for protein recognition: application to myoglobin detection, Biosens Bioelectron. 45 (2013) 237–244.
[64] S. Sadki, P. Schottland, N. Brodie, G. Sabouraud, The mechanisms of pyrrole electropolymerization, Chem Soc Rev. 29 (2000) 283–293.
[65] K.N. Kudin, B. Ozbas, H.C. Schniepp, R.K. Prud'homme, I.A. Aksay, R. Car, Raman spectra of graphite oxide and functionalized graphene sheets, Nano Lett. 8 (2008) 36–41.
[66] I. Childres, L. Jauregui, W. Park, H. Cao, Y. Chen, Raman spectroscopy of graphene and related materials, new developments in photon and materials, Research. (2013) 1–20.
[67] L.G. Cançado, A. Jorio, E.H.M. Ferreira, F. Stavale, C.A. Achete, R.B. Capaz, M.V. O. Moutinho, A. Lombardo, T.S. Kulmala, A.C. Ferrari, Quantifying defects in graphene via raman spectroscopy at different excitation energies, Nano Lett. 11 (2011) 3190–3196.
[68] S.C. Barman, A. Zahed, C. Park, S.H. Yoon, S. Zhang, H. Kim, H. Yoon, J.Y. Park, A highly selective and stable cationic polyelectrolyte encapsulated black phosphorene based impedimetric immunosensor for Interleukin-6 biomarker detection, Biosens Bioelectron. 186 (2021) 113287.
[69] P.S. Tan, E. Vaughan, J. Islam, N. Burke, D. Iacopino, J.B. Tierney, Laser scribing fabrication of graphitic carbon biosensors for label-free detection of interleukin-6, Nanomaterials. 11 (2021) 1–14.
[70] Y. Gao, D.T. Nguyen, T. Yeo, S. Bin Lim, W.X. Tan, L.E. Madden, L. Jin, J.Y. Kenan Long, F.A. Bakar Aloweni, Y.J. Angela Liew, M.L. Ling Tan, S.Y. Ang, S.D. O. Maniya, I. Abdelwahab, K.P. Loh, C.H. Chen, D.L. Becker, D. Leavesley, J.S. Ho, C.T. Lim, A flexible multiplexed immunosensor for point-of-care in situ wound monitoring, Sci Adv. 7 (2021) 1–16.
[71] M. Tertiş, B. Ciui, M. Suciu, R. Săndulescu, C. Cristea, Label-free electrochemical aptasensor based on gold and polypyrrole nanoparticles for interleukin 6 detection, Electrochim Acta. 258 (2017) 1208–1218.
[72] N. Özcan, C. Karaman, N. Atar, O. Karaman, M.L. Yola, A novel Molecularly imprinting biosensor including graphene quantum dots/multi-walled Carbon nanotubes composite for Interleukin-6 detection and electrochemical biosensor validation, ECS Journal of Solid State Science and Technology. 9 (2020) 121010.
[73] Y.T. Yaman, O.A. Vural, G. Bolat, S. Abaci, Peptide nanotubes/self-assembled polydopamine molecularly imprinted biochip for the impedimetric detection of human Interleukin-6, Bioelectrochemistry. 145 (2022) 108053.
[74] J. Liu, C.Y. Lu, H. Zhou, J.J. Xu, H.Y. Chen, Flexible gold electrode array for multiplexed immunoelectrochemical measurement of three protein biomarkers for prostate cancer, ACS Appl Mater Interfaces. 6 (2014) 20137–20143.
[75] Y. Miyao, H. Yasue, H. Ogawa, I. Misumi, T. Masuda, T. Sakamoto, E. Morita, Elevated plasma interleukin-6 levels in patients with acute myocardial infarction, Am Heart J. 126 (1993) 1299–1304.
[76] J.W. Kinney, S.M. Bemiller, A.S. Murtishaw, A.M. Leisgang, A.M. Salazar, B. T. Lamb, Inflammation as a central mechanism in Alzheimer's disease, Alzheimer's and Dementia: Translational Research and Clinical Interventions. 4 (2018) 575–590.
[77] F. Sanada, Y. Taniyama, J. Muratsu, R. Otsu, H. Shimizu, H. Rakugi, R. Morishita, Source of chronic inflammation in aging, Front Cardiovasc Med. 5 (2018) 1–5.